

# Characterization of a novel aryloxyphenoxypropionate herbicide-hydrolyzing carboxylesterase with *R*-enantiomer preference from *Brevundimonas* sp. QPT-2

Xinyun Xu, Jiahao Wang, Ting Yu, Haohan Nian, Hui Zhang\*, Guangli Wang, Feng Li

College of Life Sciences, Huaibei Normal University, Huaibei, 235000, China

## ARTICLE INFO

### Keywords:

Aryloxyphenoxypropionate herbicides  
Enantioselectivity biodegradation  
*Brevundimonas* sp.  
Carboxylesterase

## ABSTRACT

Aryloxyphenoxypropionate (AOPP) herbicides with a chiral center are widely used to selectively remove annual and perennial grasses. However, the study of the enzymes involved in enantioselective degradation of AOPP herbicides is limited. A novel family VIII carboxylesterase gene, *estwx*, hydrolyzed the ester bond cleavage of AOPP herbicides to form the corresponding acid and alkyl side chain alcohol, was cloned from *Brevundimonas* sp. strain QPT-2 and overexpressed in *E. coli* BL21. The purified recombinant EstWX was shown to hydrolyze a wide range of AOPP herbicides with various catalytic efficiencies. The enantioselectivity assay indicated that EstWX preferentially catalyzed the hydrolysis of the *R*-enantiomer of AOPP herbicides. The S73, K76, Y196 together with W368 residues, especially S73 and Y196, were essential for the catalytic function of the carboxylesterase. EstWX is a promising candidate for the bioremediation of multiple AOPP herbicide-contaminated environments and for future mechanism studies on the enantioselective degradation of chiral AOPP herbicides.

## 1. Introduction

Aryloxyphenoxypropionate (AOPP) herbicides are selective, post-emergence herbicides that share a common 4-oxyphenoxypropanoic acid ester backbone (Fig. 1) [1] and are widely used to control annual and perennial grasses in potato, sugar beet, vegetable, and other broad-leaved plant crops. AOPP herbicides are absorbed from the leaf surface and translocated throughout the plant, acting as an acetyl CoA carboxylase inhibitor [2]. The widespread application of AOPP herbicides has led to environmental pollution and aquatic ecosystem destruction [3]. Therefore, understanding the behavior and degradation of AOPP herbicides is paramount for environmental restoration.

Microbial degradation using microorganisms and enzymes for the detoxification and decontamination of AOPP herbicides is a feasible and environmentally friendly approach. Thus far, few AOPP-degrading bacterial strains have been isolated from diverse genera, including *Aquamicrobium* [4], *Acinetobacter* [5], and *Rhodococcus* [6]. Several degradation pathways of AOPP herbicides have been studied and proposed to depend on specific metabolites. *Sphingomonas paucimobilis* was shown to degrade diclofop acid to 4-(2,4-dichlorophenoxy) phenol and 2,4-dichlorophenol and/or phenol [1]. *Pseudomonas* sp. B2 was able to degrade clodinafop propargyl to clodinafop and 4-(4-chloro-2-fluorophenoxy)-phenol [7]. In addition, AOPP herbicide-hydrolyzing

carboxylesterases have also been reported, namely ChbH from *Pseudomonas azotoformans* QDZ-1 [8], AfeH from *Acinetobacter* sp. DL-2 [5], FeH from *Rhodococcus ruber* JPL-2 [6], and *Rhodococcus* sp.T1 [9].

AOPP herbicides are commonly composed of one or more chiral centers, with the resulting chiral herbicides exhibiting differing bioactivity, toxicity, and environmental fate due to their enantioselectivity [2]. Although AOPP herbicides are generally used as racemic mixtures, *R*-enantiomers exhibit higher herbicidal activity than the *S*-enantiomers [10]. The enantioselective degradation of several AOPP herbicides in soil and plant tissues has been previously reported. The *S*-enantiomer of quizalofop-P-ethyl was degraded slightly faster than the *R*-enantiomer in two soils [2]. Additionally, the *R*-enantiomers of diclofop-methyl [3] and fenoxaprop-P-ethyl [11] were found to be converted into the *S*-enantiomers in different soils, leading to the relative enrichment of the respective *R*-enantiomer. Nevertheless, to the best of our knowledge, no study has focused on the enantioselectivity of the carboxylesterases involved in the microbial metabolism of AOPP herbicides.

Herein, a novel AOPP herbicide-hydrolyzing carboxylesterase gene, *estwx*, coding for EstWX, which cleaves the AOPP ester linkage, was cloned from *Brevundimonas* sp. strain QPT-2 and functionally expressed in *E. coli* BL21 (DE3) (Novagen). The detailed biochemical characterization of EstWX was investigated and its enantioselectivity for AOPP herbicides was evaluated.

\* Corresponding author.

E-mail address: [guzhang503@sina.cn](mailto:guzhang503@sina.cn) (H. Zhang).

<https://doi.org/10.1016/j.procbio.2019.03.013>

Received 13 December 2018; Received in revised form 6 March 2019; Accepted 16 March 2019

Available online 19 March 2019

1359-5113/ © 2019 Elsevier Ltd. All rights reserved.

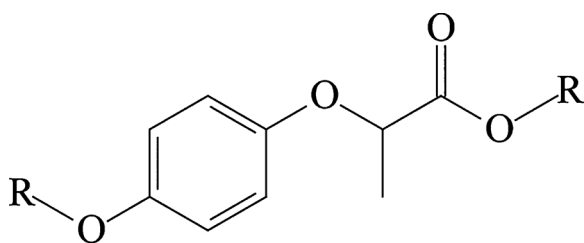


Fig. 1. Chemical structure of aryloxyphenoxypropionate (AOPP) herbicides.

## 2. Materials and methods

### 2.1. Chemicals and bacterial growth medium

Seven racemic AOPP herbicides, including quizalofop-P-tefuryl (QPT), quizalofop-P-ethyl, fenoxaprop-P-ethyl, haloxyfop-P-methyl, diclofop-methyl, cyhalofop-butyl, and fluazifop-P-butyl, were obtained from Aladdin Industrial Inc., China. Surface active agents, protease inhibitors, and all other chemicals were of analytical grade or higher purity and purchased from Shanghai Chemical Reagent Co., Ltd., China. Luria-Bertani (LB) medium (pH 7.2) and mineral salt medium (MSM) (pH 7.0) were prepared according to the method by Chen et al. [12]. The solid medium was prepared using 15 g of agar powder per liter of LB medium or MSM. The seven AOPP herbicides (10,000 mg L<sup>-1</sup>, w/v) were respectively prepared in acetone solvent.

### 2.2. Isolation and identification of AOPP herbicide-degrading bacteria

Sludge samples were collected from an AOPP herbicide-producing facility in the city of Wuhan Hubei province, China. Since QPT could produce the clearest transparent halos, thus allowing better screening of AOPP herbicide-degrading bacteria and the below positive transformants, it was selected as the substrate. After seven rounds of enrichment by MSM containing 100 mg L<sup>-1</sup> QPT as the sole carbon source, the culture was serially diluted and spread onto LB agar plates supplemented with 200 mg L<sup>-1</sup> QPT. Following incubation at 30 °C for 3 days, the colonies surrounded by transparent halos and with different morphologies were selected and further purified in LB agar plates containing 200 mg L<sup>-1</sup> QPT. One isolate, designated QPT-2, was identified based on its morphological, physiological, and biochemical properties [6] and 16S rRNA gene analysis, as previously described [13]. The phylogenetic analysis of strain QPT-2 was performed by a neighbor-joining method [14].

### 2.3. Cloning, expression of the QPT-hydrolyzing carboxylesterase gene, and protein purification

The genomic DNA was partially digested with *Sau3AI* to construct a genomic DNA library [15]. The 3–5 kb fragments were recovered and ligated into vector pUC118 (*Bam*HI/*BAP*) by T4 DNA ligase and the ligation products were transformed into *E. coli* DH5 $\alpha$ -competent cells. Transformants were smeared on LB agar plates containing 200 mg L<sup>-1</sup> of QPT and 100 mg L<sup>-1</sup> of ampicillin. Positive clones surrounded by transparent halos were selected and plasmid DNA was extracted and

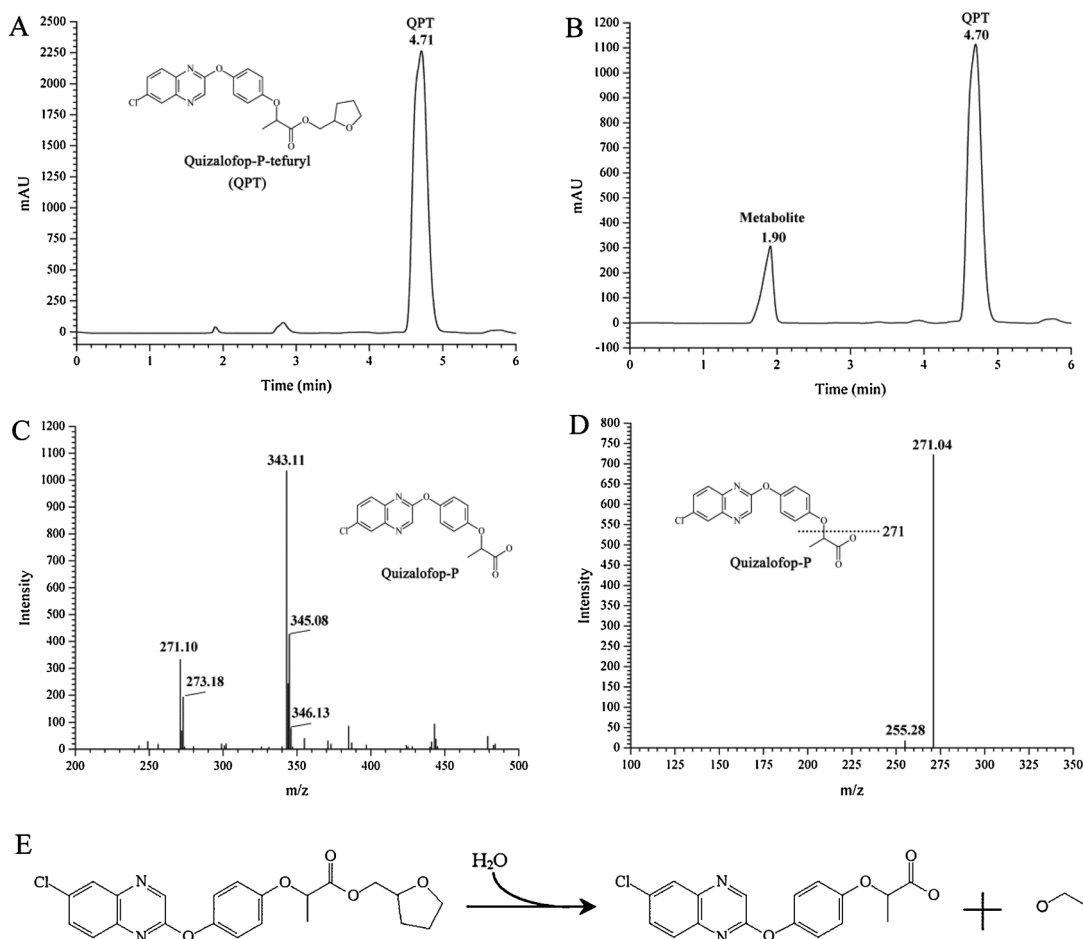
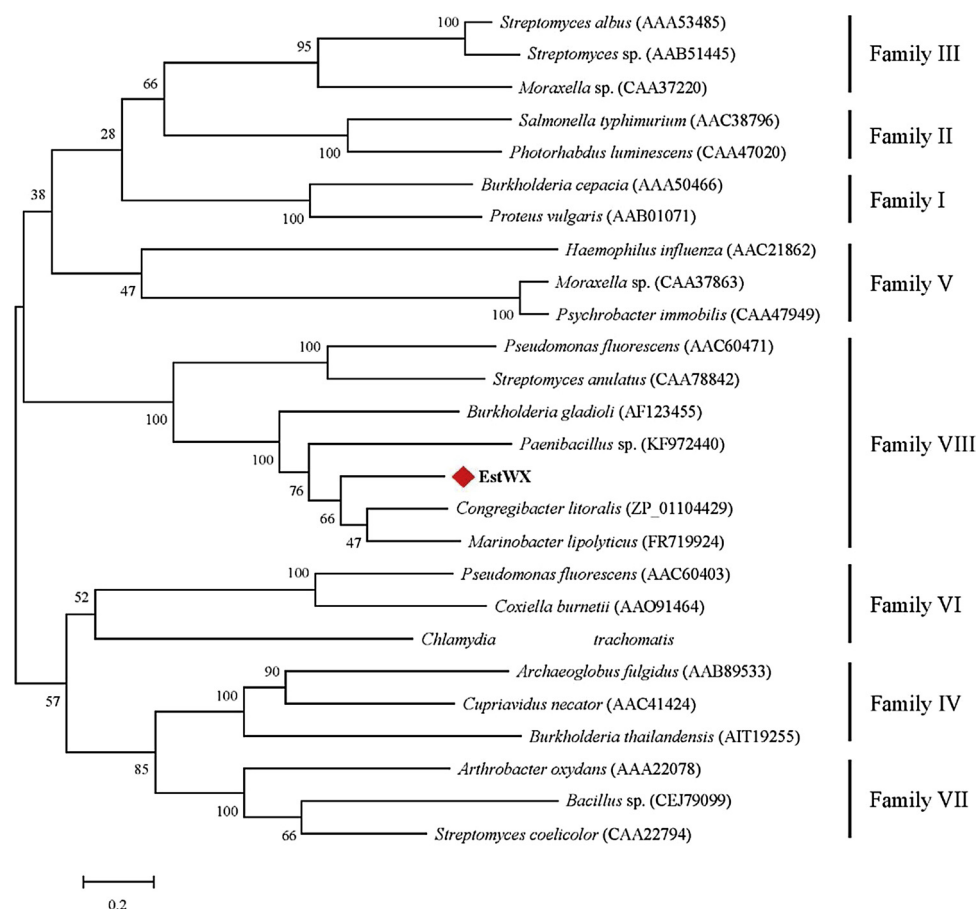


Fig. 2. LC-MS analysis of the metabolites during the QPT degradation by strain QPT-2 and a proposed metabolic pathway. (A) and (B) HPLC spectra of QPT and the QPT metabolites, respectively. (C) Mass spectrum of the QPT metabolite (RT = 1.90 min). (D) Second-order mass spectrum of  $m/z$  343  $[M-H]^-$ . (E) Proposed metabolic pathway of QPT degraded by strain QPT-2.



**Fig. 3.** Phylogenetic tree of EstWX and other related esterases from different families. GenBank accession numbers were indicated at the end of each enzyme. Phylogenetic tree was built by neighbor-joining method using MEGA 6.0 software.

sequenced. Open reading frames (ORFs) were analyzed and the predicted function of ORFs was determined using the BLASTP program provided by NCBI. A 3D model of EstWX was built using homology modelling against the crystal structure of carboxylesterase EstB (PDB ID: 1C18) [16] with SWISS-MODEL.

The *estwx* gene lacking a stop codon was amplified using the primer pair QPT-F/R (Table S1) and the resulting PCR product was ligated into pET-29a(+) vector. The recombinant plasmid, designated pET-29a-*estwx*, was transformed into *E. coli* BL21 (DE3). The colony harboring pET-29a-*estwx* was inoculated into 10 mL of LB medium containing 50 mg L<sup>-1</sup> of kanamycin and cultured overnight. Then, expression of *estwx* was induced with isopropyl β-D-1-thiogalactopyranoside (IPTG; 0.2 mM) in 100 mL of LB medium [17]. The crude enzyme extract was prepared by ultrasonic disruption and centrifugation at 10,000 g for 10 min at 4 °C after washing with PBS (pH 7.5). The supernatant was subjected to protein purification by Ni<sup>2+</sup>-NTA resin according to the instructions of the Purify Kit (Sangon Biotech, Shanghai, China), and EstWX was eluted with 200 mM imidazole. The purified EstWX was dialyzed for 3 days at 4 °C in Tris-EDTA (pH 8.0) to remove imidazole and Ni<sup>2+</sup>. SDS-PAGE and the Bradford method were used to determine the molecular mass and concentration of the protein [13].

#### 2.4. Enzymatic characterization of EstWX

The esterase activity and kinetics of purified EstWX were determined by measuring the initial rate of hydrolysis using seven AOPP herbicides as substrates [18]. The quantity of purified EstWX needed to catalyze the formation of 1 μmol of product per min under optimum conditions was defined as 1 unit (U) of enzyme activity. All assays were performed in three independent trials. For kinetic studies, the substrate

was diluted to six different concentrations (10–60 mM). Kinetic values were obtained from Lineweaver–Burk plots against various substrate concentrations.

The optimal reaction temperature, pH, thermal stability and pH stability were determined as previously described [19]. The effect of metal ions and detergents on EstWX activity was determined through the addition of various metal salts (1 mM) and detergents (1%, w/v). The effects of protein enzyme inhibitors on the activity of EstWX were estimated at final concentrations of 10 mM [17]. All tests were performed in triplicate. Enzyme activity was expressed as a percentage of the activity obtained in the absence of the exploratory factors.

#### 2.5. Chemical analysis

In liquid culture or reaction mixtures, AOPP herbicides were extracted twice with an equal volume of dichloromethane. The extracts were dried by adding anhydrous Na<sub>2</sub>SO<sub>4</sub> and the dichloromethane was evaporated under reduced pressure. The residues were dissolved in 200 μL of methanol and 10-μL samples were analyzed by an HPLC system (Agilent 1200, Agilent technologies, USA) [17]. The mobile phase consisted of methanol: water (90:10, v/v) at a flow rate of 0.8 mL min<sup>-1</sup> at 30 °C. The elution was monitored at a wavelength of 235 nm. The metabolites were identified by Liquid chromatography mass spectrometry (LC-MS) as described by Hou et al. [9].

AOPP herbicide enantioselective analysis was performed on a Chiralcel OD-H column (250 mm × 4.6 mm) using an Agilent 1200 HPLC system. The mobile phase consisted of *n*-hexane/isopropanol (85:15, v/v) at a flow rate of 1.0 mL min<sup>-1</sup> at 10 °C. The UV-vis detector wavelength was set at 235 nm and the injection volume was 10 μL. Enantioselectivity was calculated according to the method

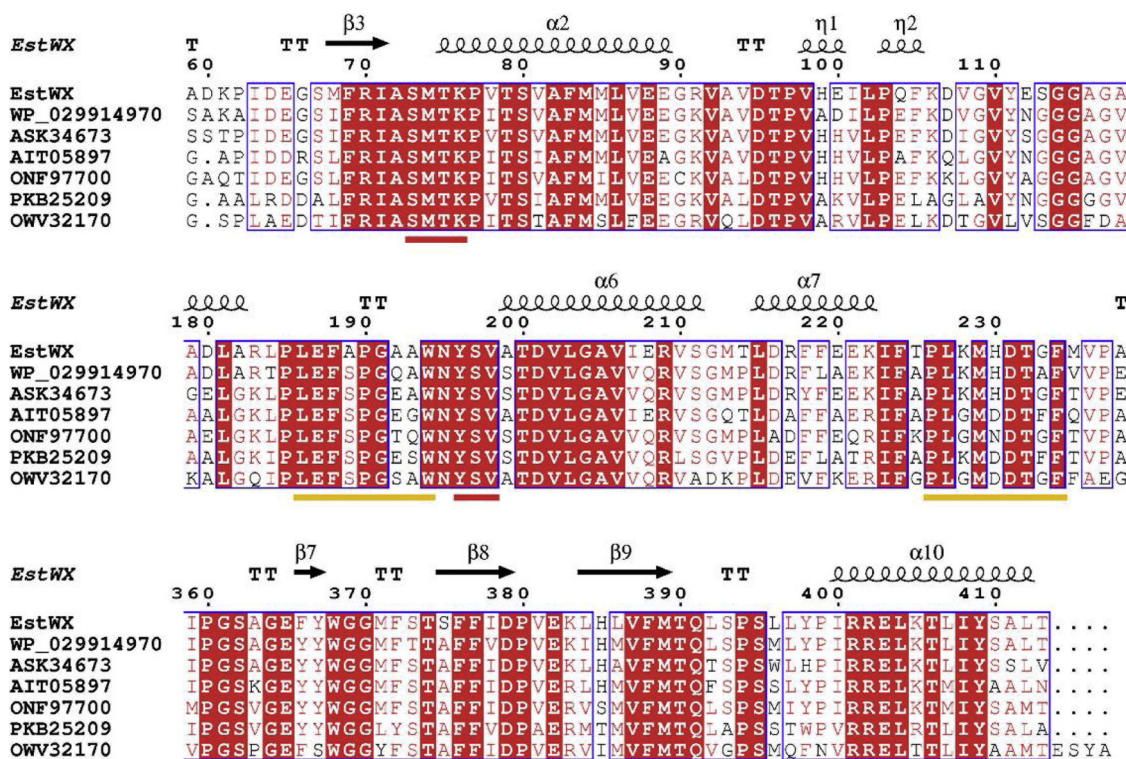


Fig. 4. Multiple alignment of amino acid sequence of EstWX and other related esterases of family VIII. WP\_029914970, serine hydrolase from *Caulobacter* sp. UNC358MFTsu5.1; ASK34673, serine hydrolase from *Alcanivorax* sp. N3-2A; AIT05897, beta-lactamase from *Sphingomonas taxi* ATCC 55669; ONF97700, esterase EstB from *Sphingomonas jeddahensis* G39; PKB25209, beta-lactamase class C family from *Novosphingobium kunmingense* CGMCC 1.12274; OWV32170, serine hydrolase from *Pacificimonas flava* JLT2012. Similar residues were shown by a clear box and identical residues were shown by a colored background. The SXXK, YSV and WGG motifs were underlined in red and LXXXPGXXW and PLGMXDTXF motifs were underlined in yellow (For interpretation of the references to colour in this figure legend, the reader is referred to the web version of this article).

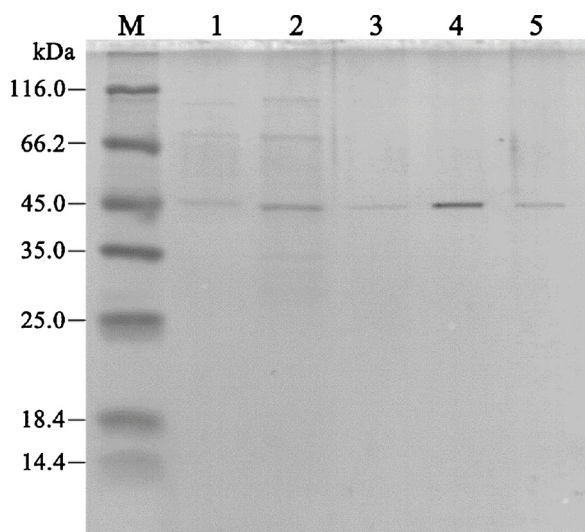


Fig. 5. SDS-PAGE analysis of the recombinant EstWX. Lane M, protein marker; lane 1–5, the purified recombinant EstWX eluted by PBS (pH 7.5) containing 20, 50, 100, 250 and 500 mM imidazole, respectively.

previously described [20]. The data were presented as averages of values at different time points over two individual experiments.

2.6. Site-directed mutagenesis of EstWX

EstWX mutants were constructed by the one-step site-directed mutagenesis protocol [17] using the high fidelity pyrobest DNA polymerase. Four pairs of mutagenic primers S73A-F/S73A-R, K76A-F/

K76A-R, Y196A-F/Y196A-R, and W368A-F/W368A-R were synthesized (Table S1) and the desired mutations were introduced in the *estwx* gene by PCR. *DpnI* was used to treat the resulting PCR products to digest the methylated template DNA. All mutation sites were confirmed by DNA sequencing. The mutant *estwx* genes were expressed following transformation into *E. coli* BL21 (DE3) and purified by the Ni<sup>2+</sup>-NTA resin Purify Kit. The enzymatic activity of the EstWX mutants was assessed as described above.

2.7. Nucleotide sequence accession numbers

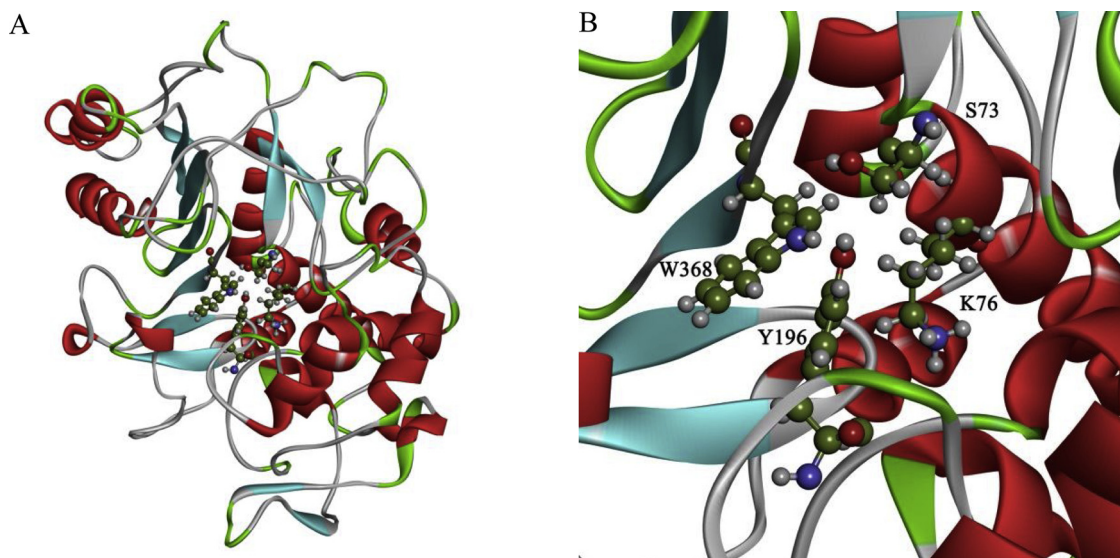
The nucleotide sequences of the 16S rRNA and *estwx* gene from strain QPT-2 have been deposited in the GenBank database under accession numbers MK560519 and MK568547, respectively.

3. Results and discussion

3.1. Isolation and identification of QPT-degrading strain

After several rounds of enrichment, strain QPT-2 exhibited the highest degradation efficiency and was selected for subsequent study. The cells of strain QPT-2 were gram-negative bacilli 1.6–3 μm in length and 0.7–1.0 μm in diameter. Basic biochemical tests indicated that strain QPT-2 was non-fermenting, aerobic, and actively motile, with a single polar flagellum. Phylogenetic analysis of the 16S rRNA gene sequence showed that strain QPT-2 was affiliated with the alphaproteobacterial genus *Brevundimonas*, sharing 98.76% identity to that of *Brevundimonas diminuta* ATCC 11568<sup>T</sup> (accession no. R775448) (Fig. S1).

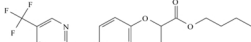
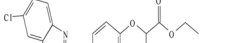
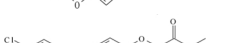
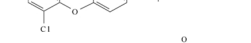
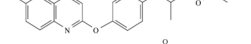
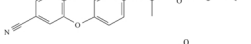
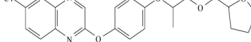
The *Brevundimonas* species are ubiquitous in the environment, being one of few bacteria with high survival rates under extremely harsh



**Fig. 6.** 3D structure model of EstWX. (A) The cartoon representation of EstWX model. The cartoon atoms for the essential catalytic residues are shown in scaled ball and stick. (B) The detailed view of the essential catalytic residues: S73, K76, Y196 and W368.

**Table 1**

Kinetic parameters of EstWX toward various AOPP herbicides.

AOPP herbicides	Molecular structure	$K_m(\mu\text{M})$	$k_{\text{cat}}(\text{s}^{-1})$	$k_{\text{cat}}/K_m$ ( $\text{s}^{-1} \text{mM}^{-1}$ )	Enzyme activity (U/mg)
QPT		$49.9 \pm 6.1$	$8.5 \pm 3.2$	170.3	$10.2 \pm 1.3$
diclofop-methyl		$39.3 \pm 3.1$	$12.9 \pm 1.2$	328.2	$15.5 \pm 1.8$
haloxyfop-P-methyl		$41.2 \pm 3.7$	$12.2 \pm 1.9$	296.1	$14.7 \pm 1.2$
fenoxaprop-P-ethyl		$51.6 \pm 4.9$	$11.4 \pm 2.1$	220.9	$13.7 \pm 1.8$
quizalofop-P-ethyl		$47.4 \pm 7.1$	$10.1 \pm 1.1$	213.7	$12.1 \pm 1.5$
cyhalofop-butyl		$48.5 \pm 5.6$	$8.2 \pm 0.6$	169.1	$9.9 \pm 1.7$
fluaizofop-P-butyl		$53.1 \pm 6.2$	$7.8 \pm 0.8$	146.9	$9.4 \pm 1.1$

**Table 2**

Enantioselectivity and conversion of EstWX for three AOPP herbicides.

Substrates	Conversion (%)	$E^{\text{(a)}}$
diclofop-methyl	69	1.5( <i>R</i> )
quizalofop-P-ethyl	53	2.2( <i>R</i> )
fluaizofop-P-butyl	42	1.7( <i>R</i> )

(a) Configuration of the preferred enantiomer is shown in parentheses.

conditions. Masoudzadeh et al. [21] isolated the bacterial strain *Brevundimonas* sp. ZF12 from an aqueous zone containing high levels of radiation, and showed that it was able to survive under high concentrations of  $\text{Cd}^{2+}$ -ion stress. Several reports are available on the degradation of environmental contaminants by members of the genus *Brevundimonas*. Strain *B. sp.* K4, isolated from activated sludge of coking wastewater, is capable of degrading quinoline, with a mean 94.8% removal efficiency prior to immobilization into reactors [22].

Wild-type *Brevundimonas* sp. LY-2 can transform the diphenyl ether herbicide lactofen to 1-(carboxy) ethyl-5-(2-chloro-4-(trifluoromethyl) phenoxy)-2-nitrobenzoate and ethanol [23]. The organophosphorus insecticide dimethoate is able to be metabolized by *Brevundimonas* sp. strain MCM B-427 [24]. Herein, strain *Brevundimonas* sp. QPT-2 was shown to be capable of degrading QPT, presenting the first documented strain of *Brevundimonas* species with the ability of degrading AOPP herbicides.

### 3.2. Identification of the metabolites during AOPP herbicide degradation by strain QPT-2

The metabolites produced during the degradation of QPT by strain QPT-2 were extracted and identified by HPLC and LC-MS. QPT and its metabolite had retention times of 4.71 and 1.90 min, respectively (Fig. 2A, B). The negative-ion chemical ionization of the metabolite (retention time = 1.90) displayed a protonated parent ion  $[\text{M}-\text{H}]^-$  at  $m/z$  343 (Fig. 2C) and a major fragment ion  $[\text{M} - \text{CH}_3\text{CH}_2\text{COOH}]^-$  at

$m/z$  271 (Fig. 2D). According to the characteristic fragment ion peaks, the QPT metabolite transformed by strain QPT-2 was identified as quizalofop-P, produced by hydrolyzing the ester bond of the tetrahydrofurfuryl alcohol moiety of QPT. These results indicate that strain QPT-2 might express an esterase to catalyze the hydrolysis of QPT to quizalofop-P and tetrahydrofurfuryl alcohol (Fig. 2E). The metabolism of QPT has been reported in goat urine [25], soil [26], and water samples [27], with quizalofop-P as the major metabolite of QPT. Additionally, quizalofop-P can be further degraded into various metabolites. Thus, since the metabolite quizalofop-P is known to be less toxic than QPT [28], the detoxification of QPT by strain QPT-2 is possible.

### 3.3. Cloning and sequence analysis of carboxylesterase gene *estwx*

A genomic DNA library of strain QPT-2 was constructed by ligation of the DNA fragments resulting from the partially digested genomic DNA into the vector pUC118. After spreading on LB agar plates supplemented with 100 mg L<sup>-1</sup> of ampicillin and 200 mg L<sup>-1</sup> of QPT, only one positive colony that produced a transparent halo was selected from among approximately 20,000 transformants. Sequence analysis indicated that the inserted fragment in the transformant was 3,020 bp long and harbored two complete ORFs, corresponding to serine hydrolase (ORF1) and TonB-dependent receptor (ORF2) encoding genes, respectively. ORF1 was then sub-cloned into the pET-28a vector and transformed into *E. coli* BL21 (DE3). The transformants were confirmed to have the ability to degrade QPT in liquid culture with induction of IPTG. Therefore, ORF1 was preliminarily identified as the target gene encoding QPT-hydrolyzing carboxylesterase and was designated as *estwx*.

The cloned *estwx* gene consists of 1,242 bp and encodes a putative protein of 413 amino acids. The putative amino acid sequence of EstWX does not match perfectly with any known proteins in the NCBI database, and only shares the highest identity (81%) with serine hydrolase (WP\_029914970) from *Caulobacter* sp. UNC358MFTsu5.1, while showing no significant identity with known carboxylesterases ChbH (ADW65729) from *Pseudomonas azotoformans* QDZ-1, AfeH (AJF83912) from *Acinetobacter baumannii* DL-2, FeH (AEK27381, AGZ87951) from *Rhodococcus* sp. T1 and *R. sp.* JPL-2. This indicates that EstWX is a novel AOPP herbicide-hydrolyzing carboxylesterase originating from a microorganism that has not yet been identified or even cultivated. Phylogenetic analysis based on multiple alignment of EstWX and other related esterases from different families revealed that EstWX was clustered as part of esterase family VIII; however, the bootstrap value in this node was only 66% (Fig. 3). Multiple alignments of amino acid sequences of EstWX with other related carboxylesterases of family VIII indicated that EstWX contains the conserved motifs SMTK, YSV, and WGG (Fig. 4), while the classical esterase/lipase family consensus motif GX SXG is absent. In addition, two motifs (LXXXPGXXW and PLGMX-DTXF) [16] that are conserved in most esterase family VIII members were also found. Based on the result of multiple alignments, it was speculated that the catalytic residues of EstWX are likely Ser-Lys-Tyr (Ser73, Lys76, and Tyr196), rather than the typical Ser-His-Asp/Glu present in most  $\alpha/\beta$ -hydrolase superfamily members [29].

### 3.4. Expression and purification of the recombinant EstWX

The recombinant EstWX with a 6×His tag at the C-terminus was overexpressed in *E. coli* BL21 (DE3) by induction with IPTG and purified by Ni<sup>2+</sup> affinity chromatography. SDS-PAGE analysis showed a single band of approximately 50 kDa, corresponding to the calculated molecular weight of the putative amino acid sequence (Fig. 5). EstWX was larger in size than those of the previously described AOPP herbicide hydrolyzing carboxylesterases, including ChbH (36 kDa) [8] and AfeH (34 kDa) [5]. The molecular weight of the native EstWX enzyme was also shown to be approximately 50 kDa by gel filtration, suggesting that this enzyme was a monomer. LC-MS analysis indicated similar

characteristic fragment ion peaks to that of QPT transformed by strain QPT-2 (Fig. S2), revealing that the recombinant EstWX was able to catalyze the hydrolysis of QPT to quizalofop-P, likely responsible for the metabolism of QPT by strain QPT-2.

### 3.5. Enzymatic characterization of EstWX

The effects of temperature and pH on the activity of EstWX were examined using QPT as a substrate. EstWX exhibited high activity at 15–50 °C, with an optimum at 40 °C (Fig. S3A), which was lower than LipBL (FR719924) from *Marinobacter lipolyticus* SM19 [30] and higher than PBS-2 (KF972440) from *Paenibacillus* sp. PBS-2 [31]. The thermal stability of EstWX was detected by incubating the enzyme for 1 h at 15–65 °C. EstWX retained > 50% of its maximal activity between 15 °C and 50 °C, and showed 33% of its maximal activity even at 65 °C, suggesting that it is a moderately thermostable enzyme. The optimal pH of EstWX at 40 °C in various buffers was assessed (Fig. S3B). EstWX retained > 60% of its maximal activity within the pH range 6.0–9.5, with optimal activity at pH 8.0. Moreover, the enzyme retained more than 60% of its activity after 1 h at pH 5.5–10.0.

The effects of metal ions on enzyme activity were measured using different metal salts at 1 mM (Fig. S3C). The enzyme activity of EstWX was obviously inhibited by more than 50% in the presence of Cu<sup>2+</sup> and Hg<sup>2+</sup>, whereas the addition of Al<sup>3+</sup>, Zn<sup>2+</sup>, and Ba<sup>2+</sup> led to the loss of 30–40% of its activity. In contrast, the activity was significantly increased to 115% and 108% in the presence of Ca<sup>2+</sup> and Mg<sup>2+</sup>, respectively. The effects of common chemical agents at concentrations of 1% were also examined (Fig. S3D). EDTA and the Ca<sup>2+</sup>-chelating agent EGTA had minimal influence on enzyme activity, suggesting that Ca<sup>2+</sup> and Mg<sup>2+</sup> might have a role in maintaining the enzyme structural stability [32] since EstWX retained a high enzyme activity in the absence of the two metal ions. A similar phenomenon was observed for other AOPP herbicide carboxylesterases, including FpbH [4] and FeH [6]. The detergents Tween-20, Tween-80, Triton-100, and SDS led to a 34–60% decline in enzyme activity. The treatment of EstWX with the histidine modifier DEPC and the thiol reagent pCMB strongly inhibited enzyme activity by more than 55%, indicating that the histidine and cysteine residues played an essential role in catalytic activity [33]. Further, an activity of only approximately 10% was detected when the serine protease inhibitor PMSF was added into the reaction mixture, revealing that the serine residues were likely involved in the formation of the catalytic sites of EstWX [34].

In order to fully assess the catalytic sites of EstWX, site-directed mutants with residue substitutions were produced as follows: S73 to A73 (S73A), K76 to A76 (K76A), Y196 to A196 (Y196A), and W368 to A368 (W368A). The enzyme assays indicated negligible activity for the mutant S73A, and less than 20% activity for the mutant Y196A, whereas mutants K76A and W368A showed 36% and 41% activity, respectively. These results are consistent with those previously reported for EstB from *Burkholderia gladioli* [16]. Thus, S73 within the SMTK motif might act as the catalytic nucleophile, in which the role of the Ser residue in family VIII is thought to be similar to that in the GX SXG motif in most of other esterase families [35]. Further, Y196 in the YSV motif may function by attacking the ester-carbonyl of AOPP herbicides, whereas the K76 in the SMTK motif and W368 in the WGG motif may contribute to the formation and stability of the catalytic complex [16,36]. Thus, S73, K76, Y196, and W368 residues in EstWX are involved in its catalytic function; this is also supported by the relative location of these four residues in the 3D model of EstWX (Fig. 6), wherein the four residues were confirmed to be located in close proximity and the hydroxyls of both S73 in the SMTK motif and Y196 in the YSV motif were pointing towards the catalytic site.

### 3.6. Substrate specificity and enantioselective activity of EstWX

The substrate specificity of EstWX was determined using various

AOPP herbicides as substrates (Table 1). EstWX exhibited a varying catalytic activity against all of tested AOPP herbicides, with the following catalytic efficiency ( $k_{cat}/K_m$ ): diclofop-methyl > haloxyfop-P-methyl > fenoxaprop-P-ethyl > quizalofop-P-ethyl > QPT > cyhalofop-butyl > fluazifop-P-butyl. The order of catalytic efficiency of EstWX for various AOPP herbicides was different from that of FpbH [4], AfeH [5], and FeH [6]. The catalytic efficiency of EstWX toward AOPP herbicides was remarkably influenced by the alkyl side chain length of the alcohol moiety, with EstWX being more susceptible to catalyzing the hydrolysis of substrates with a shorter alkyl side chain. Notably, large groups in the alkyl side chain, such as the tetrahydrofuran ring in QPT, also led to a decrease in catalytic efficiency, suggesting that the approach of EstWX to the substrates could be affected by steric hindrance [34]. The broad substrate spectrum of EstWX is expected to provide wide applications of this carboxylesterase in *in situ* bioremediation of multiple AOPP herbicide residues.

Using HPLC analysis, EstWX showed low to moderate enantioselectivity for the *R*-enantiomer of three AOPP herbicides (Table 2), implying that EstWX preferentially catalyzed the hydrolysis of the *R*-enantiomer compared to that of the *S*-enantiomer. EstCE1 from soil metagenome [37], which has a low identity (27%) with EstWX, showed high enantioselectivity for (+)-menthylacetate. Otherwise, LipBL from *Marinobacter lipolyticus* SM19 [30], Est7K from compost metagenome [29], and EstF4K from soil metagenome [38], which share moderate identity with EstWX, showed a low enantioselectivity. It is commonly known that *R*-enantiomers of AOPP herbicides have higher herbicidal activity and toxicity [39]. Further, *S*-enantiomers are degraded faster than *R*-enantiomers [2] or converted into the respective *R*-enantiomer [3] in various soils, resulting in the gradual accumulation of *R*-enantiomers in the environment and thereby leading to more potential risk for ecosystems. Since the enantioselectivity of EstWX may still be insufficient to *R*-enantiomers for environmental protection and industrial application, it is of major importance to optimize the enantioselectivity of EstWX through the construction of the mutant enzymes with amino acid substitution. In order to elucidate the mechanism of enantioselectivity, the crystal structure of the wild-type and mutant EstWX will be established and compared to determine the causes of enantioselectivity enhancement in future work. Kim et al. [40] reported that the substitution of amino acids Phe72 and Leu255 of esterase Est25 from soil metagenome significantly improved the enantioselectivity toward *S*-ketoprofen ethyl ester because the substitution of the two residues led to a change in the size of the binding pocket and entrance hole into the active site. Nevertheless, few studies have focused on the enantioselectivity of carboxylesterases involved in AOPP herbicide metabolism by microorganisms. The enantioselectivity of EstWX for the *R*-enantiomer might prove a great candidate enzyme for AOPP herbicide biodegradation where the *R*-enantiomer is the dominant contaminant. Furthermore, it may aid in the exploration of the molecular mechanisms of enantioselective recognition and enantioselective degradation of chiral herbicides. In addition, due to the tolerance to temperature, pH, metal ions, and organic solvents, as well as its broad substrate specificity and enantioselectivity, EstWX is an interesting enzyme with great potential for industrial applications such as the synthesis of chiral building blocks and resolution of racemic mixtures [41]. Immobilization is essential to improve the performance of EstWX in industrial applications. It was reported that the immobilization of LipBL on different supports increased the substrate range without affecting the enantioselectivity of the enzyme [30].

#### 4. Conclusions

A novel carboxylesterase gene, *estwx*, catalyzing the hydrolysis of AOPP herbicides to the corresponding acid and alkyl side chain alcohol, was cloned from *Brevundimonas* sp. QPT-2. The purified EstWX exhibited stability towards temperature, pH, metal ions and detergents, and had a broad substrate spectrum as well as enantioselectivity for the

*R*-enantiomer of AOPP herbicides. The S73, K76, Y196, and W368 residues were shown to be essential for the catalytic function of EstWX. Due to its low similarity with the reported carboxylesterases, the different catalytic efficiency order, and its enantioselectivity for AOPP herbicides, it is suggested that EstWX is a novel member of the AOPP herbicide-hydrolyzing carboxylesterase family. This facilitates the study on the mechanism of enantioselective recognition and enantioselective degradation of chiral AOPP herbicides in future work.

#### Author contributions

Both authors Xinyun Xu and Jiahao Wang contributed equally to this work.

#### Acknowledgements

This work was financed by grants from Provincial Natural Science Foundation of Anhui (1808085MC56), Major Program of Natural Science Research in Colleges and Universities in Anhui Province (KJ2018ZD039) and Project of outstanding young talents supporting plan in Universities of Anhui province (gxyq2018020).

#### Appendix A. Supplementary data

Supplementary material related to this article can be found, in the online version, at doi:<https://doi.org/10.1016/j.procbio.2019.03.013>.

#### References

- [1] A. Adkins, Degradation of the phenoxy acid herbicide diclofop-methyl by *Sphingomonas paucimobilis* isolated from a Canadian prairie soil, *J. Ind. Microbiol. Biotechnol.* 23 (1999) 332–335.
- [2] Z. Li, Q. Li, F. Cheng, W. Zhang, W. Wang, J. Li, Enantioselectivity in degradation and transformation of quizalofop-ethyl in soils, *Chirality* 24 (2012) 552–557.
- [3] J.L. Diao, X. Peng, W. Peng, Y.L. Lu, D.H. Lu, Z.Q. Zhou, Environmental behavior of the chiral aryloxyphenoxypropionate herbicide diclofop-methyl and diclofop: enantiomerization and enantioselective degradation in soil, *Environ. Sci. Technol.* 44 (2010) 2042–2047.
- [4] C. Wang, J. Qiu, Y. Yang, J. Zheng, H. Jian, S. Li, Identification and characterization of a novel carboxylesterase (FpbH) that hydrolyzes aryloxyphenoxypropionate herbicides, *Biotechnol. Lett.* 39 (2017) 553–560.
- [5] W. Dong, S. Jiang, K. Shi, F. Wang, S. Li, J. Zhou, F. Huang, Y. Wang, Y. Zheng, Y. Hou, Biodegradation of fenoxaprop-P-ethyl (FE) by *Acinetobacter* sp. strain DL-2 and cloning of FE hydrolase gene *afeH*, *Bioresour. Technol.* 186 (2015) 114–121.
- [6] H.M. Liu, X. Lou, Z.L. Ge, F. Yang, D.B. Chen, J.C. Zhu, J.H. Xu, S.P. Li, Q. Hong, Isolation of an aryloxyphenoxy propanoate (AOPP) herbicide-degrading strain *Rhodococcus ruber* JPL-2 and the cloning of a novel carboxylesterase gene (*feh*), *Braz. J. Microbiol.* 46 (2015) 425–432.
- [7] B. Singh, Degradation of clodinafop propargyl by *Pseudomonas* sp. strain B2, *Bull. Environ. Contam. Toxicol.* 91 (2013) 730–733.
- [8] Z.J. Nie, B.J. Hang, S. Cai, X.T. Xie, J. He, S.P. Li, Degradation of cyhalofop-butyl (CyB) by *Pseudomonas azotoformans* strain QDZ-1 and cloning of a novel gene encoding CyB-hydrolyzing esterase, *J. Agric. Food Chem.* 59 (2011) 6040–6046.
- [9] Y. Hou, J. Tao, W. Shen, J. Liu, J. Li, Y. Li, H. Cao, Z. Cui, Isolation of the fenoxaprop-ethyl (FE)-degrading bacterium *Rhodococcus* sp. T1, and cloning of FE hydrolase gene *feh*, *FEMS Microbiol. Lett.* 323 (2011) 196–203.
- [10] X. Zhang, S. Wang, Y. Wang, T. Xia, J. Chen, X. Cai, Differential enantioselectivity of quizalofop ethyl and its acidic metabolite: direct enantiomeric separation and assessment of multiple toxicological endpoints, *J. Hazard. Mater.* 186 (2011) 876–882.
- [11] Y. Zhang, D. Liu, J. Diao, Z. He, Z. Zhou, P. Wang, X. Li, Enantioselective environmental behavior of the chiral herbicide fenoxaprop-ethyl and its chiral metabolite fenoxaprop in soil, *J. Agric. Food Chem.* 58 (2010) 12878–12884.
- [12] Q. Chen, K. Chen, H. Ni, Z. Wen, H. Wang, J. Zhu, Q. He, J. He, A novel amidohydrolase (DmhA) from *Sphingomonas* sp. that can hydrolyze the organophosphorus pesticide dimethoate to dimethoate carboxylic acid and methylamine, *Biotechnol. Lett.* 38 (2016) 703–710.
- [13] J. Zhang, J.G. Yin, B.J. Hang, S. Cai, J. He, S.G. Zhou, S.P. Li, Cloning of a novel arylamidase Gene from *Paracoccus* sp. strain FLN-7 that hydrolyzes amide pesticides, *Appl. Environ. Microbiol.* 78 (2012) 4848–4855.
- [14] G. Altarescu, T. Eldar-Geva, B. Brooks, E. Zylber-Haran, I. Varshaver, E.J. Margalioth, E. Levy-Lahad, P. Renbaum, Preimplantation genetic diagnosis (PGD) for nonsyndromic deafness by polar body and blastomere biopsy, *J. Assist. Reprod. Genet.* 26 (2009) 391–397.
- [15] Z. Yi, K. Li, J. Song, Y. Shi, Y. Yan, Molecular cloning, purification and biochemical characterization of a novel pyrethroid-hydrolyzing carboxylesterase gene from *Ochrobactrum anthropi* YZ-1, *J. Hazard. Mater.* 221–222 (2012) 206–212.

- [16] U.G. Wagner, E.I. Petersen, H. Schwab, C. Kratky, EstB from *Burkholderia gladioli*: a novel esterase with a beta-lactamase fold reveals steric factors to discriminate between esterolytic and beta-lactam cleaving activity, *Protein Sci.* 11 (2002) 467–478.
- [17] H. Zhang, M.Y. Li, J. Li, G.L. Wang, F. Li, D.Y. Xu, Y. Liu, M.H. Xiong, A key esterase required for the mineralization of quizalofop-p-ethyl by a natural consortium of *Rhodococcus* sp. JT-3 and *Brevundimonas* sp. JT-9, *J. Hazard. Mater.* 327 (2017) 1–10.
- [18] X. Wang, X. Geng, Y. Egashira, H. Sanada, Purification and characterization of a feruloyl esterase from the intestinal bacterium *Lactobacillus acidophilus*, *Appl. Environ. Microbiol.* 70 (2004) 2367–2372.
- [19] J.K. Rhee, D.G. Ahn, Y.G. Kim, J.W. Oh, New thermophilic and thermostable esterase with sequence similarity to the hormone-sensitive lipase family, cloned from a metagenomic library, *Appl. Environ. Microbiol.* 71 (2005) 817–825.
- [20] E. Henke, U.T. Bornscheuer, R.D. Schmid, J. Pleiss, A molecular mechanism of enantioselective recognition of tertiary alcohols by carboxylesterases, *ChemBiochem* 4 (2003) 485–493.
- [21] N. Masoudzadeh, L. Alidoust, N. Samie, H. Hajfarajollah, H. Sharafi, S. Modiri, H.S. Zahiri, H. Vali, K.A. Noghabi, Distinctive protein expression patterns of the strain *Brevundimonas* sp. ZF12 isolated from the aqueous zone containing high levels of radiation to cadmium-induced stress, *J. Biotechnol.* 186 (2014) 49–57.
- [22] C. Wang, M. Zhang, F. Cheng, Q. Geng, Biodegradation characterization and immobilized strains' potential for quinoline degradation by *Brevundimonas* sp. K4 isolated from activated sludge of coking wastewater, *Biosci. Biotechnol. Biochem.* 79 (2015) 164–170.
- [23] B. Liang, Y. Zhao, P. Lu, S. Li, X. Huang, Biotransformation of the diphenyl ether herbicide lactofen and purification of a lactofen esterase from *Brevundimonas* sp. LY-2, *J. Agric. Food Chem.* 58 (2010) 9711–9715.
- [24] N.M. Deshpande, S.S. Sarnaik, S.A. Paranjpe, P.P. Kanekar, Optimization of dimethoate degradation by *Brevundimonas* sp. MCM B-427 using factorial design: studies on interactive effects of environmental factors, *World J. Microb. Biot.* 20 (2004) 455–462.
- [25] A.R. Banijamali, R.J. Strunk, J.K. Nag, G.J. Putterman, M.H. Gay, Identification of [14C]quizalofop-P-tefuryl metabolites in goat urine by nuclear magnetic resonance and mass spectrometry, *J. Agric. Food Chem.* 41 (1993) 1122–1128.
- [26] R. López-Ruiz, R. Romero-González, J.L. Martínez Vidal, M. Fernández-Pérez, F.A. Garrido, Degradation studies of quizalofop-p and related compounds in soils using liquid chromatography coupled to low and high resolution mass analyzers, *Sci. Total Environ.* 607–608 (2017) 204–213.
- [27] R. López-Ruiz, R. Romero-González, J.L. Martínez Vidal, F.A. Garrido, Behavior of quizalofop-p and its commercial products in water by liquid chromatography coupled to high resolution mass spectrometry, *Ecotoxicol. Environ. Saf.* 157 (2018) 285–291.
- [28] A.C. Belfroid, M. van Drunen, M.A. Beek, S.M. Schrap, C.A.M. van Gestel, B. van Hattum, Relative risks of transformation products of pesticides for aquatic ecosystems, *Sci. Total Environ.* 222 (1998) 167–183.
- [29] H.W. Lee, W.K. Jung, Y.H. Kim, B.H. Ryu, T.D. Kim, J. Kim, H. Kim, Characterization of a novel alkaline family VIII esterase with S-enantiomer preference from a compost metagenomic library, *J. Microbiol. Biotechnol.* 26 (2016) 315–325.
- [30] D. Pérez, S. Martín, G. Fernández-Lorente, M. Filice, J.M. Guisán, A. Ventosa, M.T. García, E. Mellado, A novel halophilic lipase, LipBL, showing high efficiency in the production of eicosapentaenoic acid (EPA), *PLoS One* . 6 (2011) e23325.
- [34] B. Wang, P. Guo, B. Hang, L. Li, J. He, S. Li, Cloning of a novel pyrethroid-hydrolyzing carboxylesterase gene from *Sphingobium* sp. Strain JZ-1 and characterization of the gene product, *Appl. Environ. Microbiol.* 75 (2009) 5496–5500.
- [35] Y. Hu, Y. Liu, J. Li, Y. Feng, N. Lu, B. Zhu, S. Xue, Structural and functional analysis of a low-temperature-active alkaline esterase from South China Sea marine sediment microbial metagenomic library, *J. Ind. Microbiol. Biotechnol.* 42 (2015) 1449–1461.
- [36] K. Rashamuse, V. Magomani, T. Ronneburg, D. Brady, A novel family VIII carboxylesterase derived from a leachate metagenome library exhibits promiscuous  $\beta$ -lactamase activity on nitrocefin, *Appl. Microbiol. Biotechnol.* 83 (2009) 491–500.